Journal of Marine Science and Technology
DOI: 10.6119/JMST-013-0207-4

Combined effects of magnetic field and surface roughness on long journal bearing lubricated with ferrofluid

Tze-Chi Hsu[1], Jing-Hong Chen[1], Hsin-Lu Chiang[2], and Tsu-Liang Chou[2]

Key words: ferrofluid, long journal bearing, stochastic surface roughness.

ABSTRACT

This study investigated the influence of ferrofluids on the lubrication performance of long journal bearings under the combined effects of stochastic surface roughness and a magnetic field generated by an infinitely long wire. According to our results, placing an infinitely long wire magnetic field at an appropriate distance from the center of the bearing can suppress side leakage in long journal bearings, thereby extending the life of the bearings. Under a higher power-law index and induced magnetic force, the introduction of transverse roughness can enhance film pressure and load capacity, while reducing the attitude angle and modified friction coefficient. The introduction of longitudinal roughness has the opposite effect. We believe that these findings provide a valuable reference for the design of bearings in the future.

I. INTRODUCTION

Ferrofluids are stable colloidal liquids comprising ferromagnetic particles suspended within a carrier fluid. Special attention must be paid to the non-Newtonian characteristics of ferrofluids under various operating environments [6, 9-11, 14, 18-20, 22]. Nada and Osman [13] and Osman et al. [15-17] investigated the influence of ferrofluid lubricants on the operational characteristics of journal bearings, using specifically designed magnetic field models. Their results indicate that increasing the power law index of ferrofluids and the intensity of the magnetic field can enhance the load capacity and attitude angle of the bearings, while decreasing the modified friction coefficient in cases of high eccentricity. However, the model used to determine the applied magnetic field must be selected with care to avoid causing side leakage due to excessive film pressure. Other similar studies include those by Montazeri [12], and Huang et al. [8].

The above studies all assumed that the surfaces within bearings are entirely smooth. Christensen [4] and Christensen and Tonder [5] developed stochastic Reynolds equations to describe average pressure, addressed the issue of transverse and longitudinal roughness, and determined the influence of roughness on the performance of bearings. Chiang et al. [1-3] derived a generalized stochastic Reynolds equation based on Christensen's stochastic model and the Stokes microcontinuum theory [20]. Through numerical simulation, the performance of lubrication in bearings under the combined influence of couple stresses and surface roughness was determined in order to characterize the dynamic squeeze film. Hsu et al. [7] applied Christensen's stochastic roughness theory to the problem of two parallel circular disks, the results of which demonstrate that surface roughness could improve the behavior of squeeze films. Magnetic particles are often trapped in the valleys associated with surface roughness; therefore, Chu et al. [6] and Osman et al. [16-17] used the power-law flow model as the rheology model for ferrofluid characteristics. Nonetheless, previous studies have tended to focus on the impact of surface roughness or ferrofluids, without considering the influence of magnetic fields. The objective of the current study was to investigate the combined effects of surface roughness and ferrofluid characteristics as well as magnetic fields.

This study combined Christensen's stochastic surface

Paper submitted 10/11/12; revised 01/18/13; accepted 02/07/13. Author for correspondence: Jing-Hong Chen (e-mail: jinghong@seed.net.tw).

[1]Department of Mechanical Engineering, Yuan-Ze Unversity, Chung-Li, Taiwan, R.O.C.

[2]Department of Mechanical Engineering, Taoyuan Innovation Institute of Technology, Chung-Li, Taiwan, R.O.C.

Nomenclature

c	one half of the total range of the random film thickness variable	n	power-law index
		P_m	induced magnetic pressure
C	radial clearance	$\overline{p}$, P	mean film pressure, $P=\left(\overline{p}/m_0\omega^n\right)(C/R)^{n+1}$
e	eccentricity, $e=\varepsilon C$	R	radius of the journal
f_{mx}	magnetic forces in x-direction (circumferential d direction)	X_m	susceptibility of ferrofluid
f_{mz}	magnetic forces in z-direction (axial direction)	x, y, z	rectangular coordinates
h_M	magnetic field intensity	Z	dimensionless coordinate in the z-direction, Z=z / L
h_{M0}	characteristic value of magnetic field intensity	α_m	magnetic field coefficient, $\alpha_m=\left(h_{M0}^2\mu_0 X_m/m_0\omega^n\right)(C/R)^{n+1}$
H_M	dimensionless magnetic field intensity, $H_M=h_M/h_{M0}$	ε	eccentricity ratio, $\varepsilon=e/C$
h	thickness of lubricant film	δ	random part of film geometry
h_m, H	nominal smooth part of the film thickness, $H=h_m/C=1+\varepsilon\cos\theta$	θ	circumferential coordinate, $x=R\theta$
		θ_2	zero-pressure gradient angle
K	distance ratio parameter $K=R_0/R$	λ	length-to-diameter, $\lambda=L/2R$
L	length of the bearing	Λ	roughness parameter, $\Lambda=c/C$
m_0	viscosity constant	μ_0	permeability of free space of air, $\mu_0=4\pi\times10^{-7}$ AT/m
		ω	angular speed

roughness model with a magnetic field generated using an infinitely long wire and investigated how this would affect bearings lubricated with ferrofluids. It is hoped that this comprehensive research on the lubrication performance of hydrodynamic bearings will provide a valuable reference for the design of bearing in the future.

II. THEORETICAL ANALYSIS

Figure 1 depicts the configuration of a long bearing with a journal radius R rotating at angular speed ω, with the lubrication of the interior bearings provided by ferrofluid. A magnetic field is produced by a current passing through an infinitely long wire, which is displaced at a distance (R0) greater than the radius of the bearing. The wire is placed at angle ψ from the centerline of the bearing.

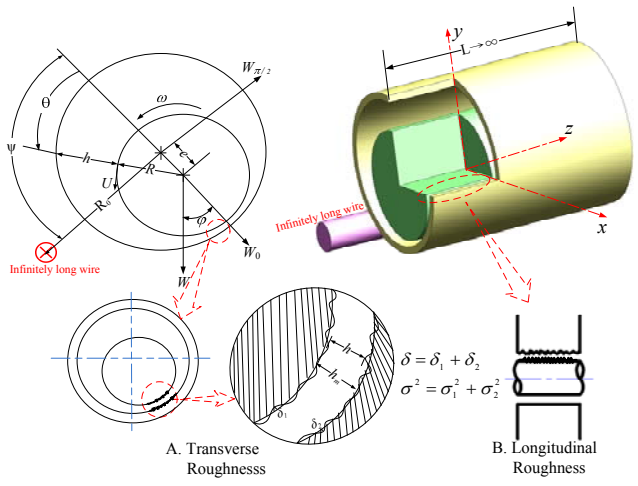

Fig. 1. The frame structure of the transmitted bit stream.

In accordance with the Navier-Stokes equation, magnetic force was treated as an external body force and the modified Reynolds equation was then obtained as [13]

$$\frac{\partial}{\partial x}\left(\frac{h^{n+2}}{n}\frac{\partial p}{\partial x}\right)+\frac{\partial}{\partial z}\left(h^{n+2}\frac{\partial p}{\partial z}\right)=6m_0(R\omega)^n\frac{\partial h}{\partial x}+\frac{\partial}{\partial x}\left(\frac{h^{n+2}}{n}f_{MX}\right)+\frac{\partial}{\partial z}\left(h^{n+2}f_{MZ}\right) \quad (1)$$

where n is the power-low index, p is local film pressure, and m_0 is the viscosity constant. The f_{MX} and f_{MZ} respectively represent magnetic force in the circumferential and axial directions, written as follows:

$$f_{MX}=\mu_0 X_M h_M\frac{\partial h_M}{\partial x} \quad (2)$$

$$f_{MZ}=\mu_0 X_M h_M\frac{\partial h_M}{\partial z} \quad (3)$$

The magnetic field h_M of the infinitely wire long [13] is represented by

$$h_M(\theta)=\frac{I}{2\pi R}\left(1+K^2-2K\cos\{\psi-\theta\}\right)^{-0.5} \quad (4)$$

where I is the strength of the current passing through the wire and $K=R_0/R$.The optimum ψ , as given by Tarapov [21] is π/2.

According to Christensen's theory, using the expected values derived from Eq. (1), the stochastic modified Reynolds equation for the journal bearing with rough surface can be written as:

$$\frac{\partial}{\partial x}\left[E\left(\frac{h^{n+2}}{n}\right)\frac{\partial p}{\partial x}\right]+\frac{\partial}{\partial z}\left[E\left(h^{n+2}\right)\frac{\partial p}{\partial z}\right]=6m_0(R\omega)^n\frac{\partial E(h)}{\partial x}+\frac{\partial}{\partial x}\left[E\left(\frac{h^{n+2}}{n}\right)f_{MX}\right]+\frac{\partial}{\partial z}\left(E\left(h^{n+2}\right)f_{MZ}\right) \quad (5)$$

where the expectancy operator $E(\cdot)$ is defined by

$$E(\cdot)=\int_{-\infty}^{\infty}(\cdot)f(\delta)d\delta \quad (6)$$

and $f(\delta)$ is the probability density distribution for the stochastic variables. As most rough surfaces in the field of engineering are Gaussian in nature, for the sake of simplicity, we used a polynomial form for integration (instead of a Gaussian

distribution function), as shown in the following:

$$f(\delta)=\begin{cases}\dfrac{35}{32c^7}\left(c^2-\delta^2\right)^3 & if\ -c\le\delta\le c\\ 0 & elsewhere\end{cases} \tag{7}$$

where c is the half total range of random film thickness variable and, the function terminates at $c = \pm 3\sigma$, where σ is the standard deviation.

In this study, local film geometry of the lubricant is treated as a stationary, ergodic, stochastic process with zero mean, written as follows:

$$h = h_m(x,z) + \delta(x,z,\xi) \tag{8}$$

where h_m represents the nominal smooth part of the film geometry according to the x and z coordinates, while $\delta(x,z,\xi)$ is the part due to the surface asperities measured from the nominal level and is regarded as a randomly varying quantity of zero mean. Using the circumferential coordinate, film thickness h_m can also be expressed as

$$h_m = C(1+\varepsilon\cos\theta) \tag{9}$$

where C is the radial clearance, and ε is eccentricity ratio, $\varepsilon = e/C$.

The surface feature of one-dimensional longitudinal roughness is assumed to have the form of long narrow ridges and valleys running in the direction of rotation. Thus, the thickness of the lubricating film listed in Eq. (8) can be expressed as a function of the form

$$h = h_m(x) + \delta(x,\xi) \tag{10}$$

in which Eq. (5), dealing with longitudinal roughness, can be reduced to

$$\frac{\partial}{\partial x}\left[E\left(\frac{h^{n+2}}{n}\right)\frac{\partial\bar{p}}{\partial x}\right]+\frac{\partial}{\partial z}\left[\frac{1}{E\left(1/h^{n+2}\right)}\frac{\partial\bar{p}}{\partial z}\right]=6m_0(R\omega)^n\frac{\partial E(h)}{\partial x}+\frac{\partial}{\partial x}\left[E\left(\frac{h^{n+2}}{n}\right)f_{MX}\right]+\frac{\partial}{\partial z}\left(\frac{1}{E\left(1/h^{n+2}\right)}f_{MZ}\right) \tag{11}$$

where $\bar{p}$ is mean film pressure.

To simplify analysis, the magnetic field coefficient can be defined as

$$\alpha_m = \frac{h_{M0}^2\mu_0 X_M}{m_0\omega^n}\left(\frac{C}{R}\right)^{n+1} \tag{12}$$

while dimensionless mean film pressure P and surface roughness parameter Λ, are written as

$$P = \frac{\bar{p}}{m_0\omega^n}\left(\frac{C}{R}\right)^{n+1} \tag{13}$$

$$\Lambda = \frac{c}{C} \tag{14}$$

The non-dimensional modified Reynolds equation for longitudinal roughness can then be expressed as follows:

$$\begin{aligned}\frac{\partial}{\partial\theta}\left[G_1(H,\Lambda,n)\frac{\partial P}{\partial\theta}\right]+\frac{n}{4\lambda^2}\frac{\partial}{\partial Z}\left[G_2(H,\Lambda,n)\frac{\partial P}{\partial Z}\right]&=6n\frac{\partial H}{\partial\theta}\\ +\alpha_m\frac{\partial}{\partial\theta}\left[G_1(H,\Lambda,n)H_M\frac{\partial H_M}{\partial\theta}\right]&+\frac{n\alpha_m}{4\lambda^2}\frac{\partial}{\partial Z}\left[G_2(H,\Lambda,n)H_M\frac{\partial H_M}{\partial Z}\right]\end{aligned} \tag{15}$$

Where

$$H = \frac{h_m}{C} \tag{16}$$

$$Z = z/L \tag{17}$$

$$\lambda = \frac{L}{2R} \tag{18}$$

$$\theta = x/R \tag{19}$$

$$G_1(H,\Lambda,n) = H^{n+2}+\frac{1}{18}H^n\Lambda^2\left(n^2+3n+2\right) \tag{20}$$

$$G_2(H,\Lambda,n) = \frac{1}{H^{n+2}}+\frac{\Lambda^2\left[n^2+5n+6\right]}{18\cdot H^{n+4}} \tag{21}$$

and the intensity of the dimensionless magnetic field of Eq. (4) can be written as

$$H_M(\theta) = \left(1+K^2-2K\cos\{\psi-\theta\}\right)^{-0.5} \tag{22}$$

where

$$H_M = h_M/h_{M0} \tag{23}$$

and $h_{M0} = I/2\pi R$ (24)

One-dimensional transverse roughness is assumed to have the form of long narrow ridges and valleys running in the z direction. Therefore, the thickness of the lubricant film can be expressed as a function of the form:

$$h = h_m(x)+\delta(z,\xi) \tag{25}$$

Equation (15) for transverse roughness can be derived as

$$\begin{aligned}&\frac{\partial}{\partial\theta}\left[G_2(H,\Lambda,n)\frac{\partial P}{\partial\theta}\right]+\frac{n}{4\lambda^2}\frac{\partial}{\partial Z}\left[G_1(H,\Lambda,n)\frac{\partial P}{\partial Z}\right]\\ &=6n\frac{\partial}{\partial\theta}G_3(H,\Lambda,n)+\alpha_m\frac{\partial}{\partial\theta}\left[G_2(H,\Lambda,n)H_M\frac{\partial H_M}{\partial\theta}\right]\\ &+\frac{n\alpha_m}{4\lambda^2}\frac{\partial}{\partial Z}\left[G_1(H,\Lambda,n)H_M\frac{\partial H_M}{\partial Z}\right]\end{aligned} \tag{26}$$

where

$$G_3(H,\Lambda,n) = H\cdot\frac{18H^2+\Lambda^2\left[n^2+5n+6\right]}{18H^2+\Lambda^2\left[n^2+7n+12\right]} \tag{27}$$

Because $\lambda >> 5$ in the approximation of a long journal bearing, variations in axial pressure can be disregarded in favor of circumferential variations. Therefore, Eqs. (15) and (26) are reduced to

$$\begin{aligned}&\frac{\partial}{\partial\theta}\left[G_1(H,\Lambda,n)\frac{\partial P}{\partial\theta}\right]=6n\left(-\varepsilon\cdot\sin\theta\right)\\ &+\alpha_m\frac{\partial}{\partial\theta}\left[G_1(H,\Lambda,n)H_M(\theta)\frac{\partial H_M(\theta)}{\partial\theta}\right]\end{aligned}\quad \text{Longitudinal} \tag{28}$$

$$\frac{\partial}{\partial\theta}\left[G_2(H,\Lambda,n)\frac{\partial P}{\partial\theta}\right]=6n\frac{\partial}{\partial\theta}G_3(H,\Lambda,n)$$
$$+\alpha_m\frac{\partial}{\partial\theta}\left[G_2(H,\Lambda,n)\cdot H_M(\theta)\cdot\frac{\partial H_M(\theta)}{\partial\theta}\right]\quad\text{Transverse}\qquad(29)$$

The boundary conditions for film pressure are as follows:

$$P(\theta)=0\quad\text{at}\quad\theta=0\qquad(30)$$

$$\frac{dP}{d\theta}=0\quad\text{at}\quad\theta=\theta_2\qquad(31)$$

By applying boundary conditions (30) and (31), the non-dimensional mean film pressure and θ_2 can be obtained by integrating Eqs. (28) and (29) as

$$P(\theta)=$$
$$\begin{cases}6\cdot\varepsilon\cdot n\cdot\int_0^{\theta}\frac{(\cos\theta-\cos\theta_2)}{G_1(H,\Lambda,n)\big|_\theta}\cdot d\theta+\alpha_m\cdot R(\psi,\theta,K)\\ \quad-\alpha_m\cdot\left[G_1(H,\Lambda,n)\cdot Q(\psi,\theta,K)\right]_{\theta_2}\cdot\int_0^{\theta}\frac{1}{G_1(H,\Lambda,n)\big|_\theta}\cdot d\theta\\ \qquad\qquad\text{Longitudinal}\qquad(32)\\ 6n\cdot\int_0^{\theta}\left[G_3(H,\Lambda,n)\big|_\theta-G_3(H,\Lambda,n)\big|_{\theta_2}\right]\cdot G_4(H,\Lambda,n)\cdot d\theta\\ \quad+\alpha_m\cdot R(\psi,\theta,K)-\alpha_m\cdot\left[G_2(H,\Lambda,n)\cdot Q(\psi,\vartheta,K)\right]_{\theta_2}\cdot\int_0^{\theta}G_4(H,\Lambda,n)\cdot d\theta\\ \qquad\qquad\text{Transverse}\qquad(33)\end{cases}$$

$$\cos\theta_2=$$
$$\begin{cases}\dfrac{6\cdot\varepsilon\cdot n\cdot\int_0^{\theta_2}\frac{\cos\theta}{G_1(H,\Lambda,n)\big|_\theta}\cdot d\theta+\alpha_m\cdot\left[R(\psi,\theta,K)\right]}{6\cdot\varepsilon\cdot n\cdot\int_0^{\theta_2}\frac{1}{G_1(H,\Lambda,n)\big|_\theta}\cdot d\theta}\\ \qquad-\dfrac{\alpha_m\cdot\left[G_1(H,\Lambda,n)\cdot Q(\psi,\theta,K)\right]_{\theta_2}\cdot\int_0^{\theta_2}\frac{1}{G_1(H,\Lambda,n)\big|_\theta}\cdot d\theta}{6\cdot\varepsilon\cdot n\cdot\int_0^{\theta_2}\frac{1}{G_1(H,\Lambda,n)\big|_\theta}\cdot d\theta}\\ \qquad\qquad\text{Longitudinal}\qquad(34)\\ \dfrac{6n\cdot\left\{\int_0^{\theta_2}\left(G_3(H,\Lambda,n)\big|_\theta\right)\cdot G_4(H,\Lambda,n)\cdot d\theta\right\}+\alpha_m\cdot R(\psi,\theta,K)}{6n\cdot\theta_2\cdot\varepsilon\cdot\int_0^{\theta_2}G_5(H,\Lambda,n)\cdot G_4(H,\Lambda,n)\cdot d\theta}\\ \qquad-\dfrac{\alpha_m\cdot\left[G_1(H,\Lambda,n)\cdot Q(\psi,\theta,K)\right]_{\theta_2}\cdot\int_0^{\theta}G_4(H,\Lambda,n)\big|\cdot d\theta}{6n\cdot\theta_2\cdot\varepsilon\cdot\int_0^{\theta_2}G_5(H,\Lambda,n)\cdot G_4(H,\Lambda,n)\cdot d\theta}-\dfrac{1}{\varepsilon}\\ \qquad\qquad\text{Transverse}\qquad(35)\end{cases}$$

where

$$G_4(H,\Lambda,n)=\frac{1}{H^{n+2}}+\frac{\Lambda^2\left[n^2+5n+6\right]}{18\cdot H^{n+4}}\qquad(36)$$

$$G_5(H,\Lambda,n)=\frac{18H^2+\Lambda^2\left(n^2+5n+6\right)}{18H^2+\Lambda^2\left(n^2+7n+12\right)}\Bigg|_{\theta_2}\qquad(37)$$

$$R(\psi,\theta,K)=\frac{1}{2}\cdot\left[H_M^2(\theta)-H_M^2(0)\right]\qquad(38)$$

$$Q(\psi,\theta,K)=\frac{\left(1+K^2-2K\cos\{\psi-\theta\}\right)^{-0.5}\cdot K\cdot\sin(\psi-\theta)}{\left(1+K^2-2K\cos\{\psi-\theta\}\right)^{-1.5}}\qquad(39)$$

By integrating the non-dimensional mean film pressure acting on the journal bearing, the dimensionless load components parallel (W_0) and perpendicular ($W_{\pi/2}$) to the centerline can be obtained by the following:

$$W_0=-2\int_0^{\theta_2}\int_0^{\frac{1}{2}}P(\theta)\cos\theta dZd\theta\qquad(40)$$

$$W_{\pi/2}=2\int_0^{\theta_2}\int_0^{\frac{1}{2}}P(\theta)\sin\theta dZd\theta\qquad(41)$$

Thereafter, dimensionless load capacity W and attitude angle φ can be evaluated from the above, as follows:

$$W=\left[W_0^2+W_{\pi/2}{}^2\right]^{1/2}\qquad(42)$$

$$\varphi=\tan^{-1}\left[W_{\pi/2}/W_0\right]\qquad(43)$$

Shear stress on the moving surface in the direction of rotation can also be calculated, such that the modified friction coefficient f R/C is determined by

$$f\frac{R}{C}=\frac{2\int_0^{\frac{1}{2}}\int_0^{2\pi}\frac{1}{H^n}\cdot\left(1+\gamma\cdot\frac{\partial P(\theta)}{\partial\theta}-\gamma\cdot\alpha_m\cdot Q(\psi,\theta,K)\right)^n d\theta dZ}{W}\qquad(44)$$

where

$$\gamma=\frac{(1+\varepsilon\cos\theta)^{n+1}}{2n}\qquad(45)$$

III. RESULTS AND DISCUSSION

This study investigated the combined influence of surface roughness patterns and a magnetic field produced by an infinitely long wire on the distribution of hydrodynamic pressure in long journal bearings lubricated with ferrofluids. Figure 2 depicts the impact of various magnetic field coefficients on dimensionless pressure distribution under smooth surface conditions. The coefficient of the magnetic field in this study was 4 λ^2 times that of the coefficient used by Osman [12] (i.e., α_m=4 $\lambda^2\alpha$). Clearly, P_{max} increases with the coefficient of the magnetic field. However, excessively high and concentrated dimensionless pressure was found to cause side leakage, thereby reducing the operational life of the bearing. In seeking to address this defect, we discovered that the relative location of the metal wire has an absolute impact on the distribution of dimensionless pressure (Fig. 3). When K was increased from 1.2 to 3, P_{max} decreased significantly. Taking K=3 as an example, dimensionless pressure increased steadily from θ=0 to the maximum value and then swiftly dropped to zero. This is considered by many scholars to be the ideal curve.

Figure 4 compares the simulation results of this study and those of Chiang [2]. Under a magnetic force of 0, our numerical results were similar to those obtained by Chiang, demonstrating that an increase in the magnetic field contributed to an increase in dimensionless pressure. Using α_m=5 as an example, com-

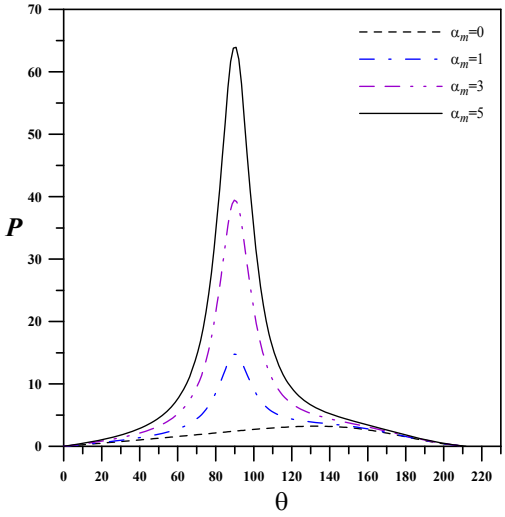

Fig. 2. Numerical analysis of α_m influence on dimensionless pressure (Z=0, n=1, ε=0.4 , Λ=0, λ=5, K=1.2)

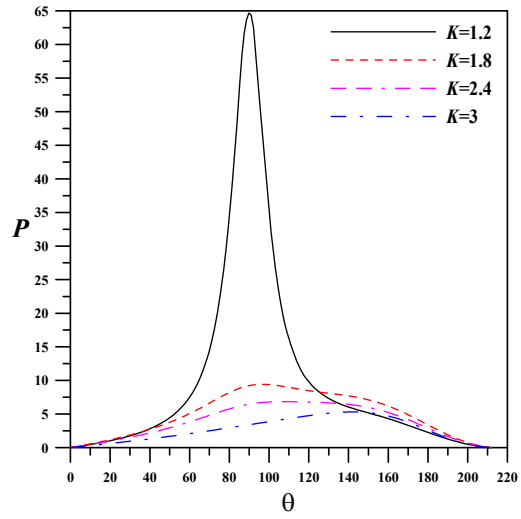

Fig. 3. Numerical analysis of K influence on dimensionless pressure (Z=0, n=1, ε=0.4, Λ=0, λ=5, α_m=5)

pared to a smooth bearing surface, transverse roughness increased P_{max} whereas longitudinal roughness decreased P_{max}.

Although the viscosity of ferrofluids changes only slightly in the Schliomis model, a number of studies [6, 16−17] have shown that viscosity can be affected by differences in the weight ratio of ferromagnetic particles within the fluid. Therefore, the impact of various power law indices on dimensionless pressure distribution under the influence of surface roughness is shown in Fig. 5. Observation revealed that with a fixed power law index, surface roughness has a significant influence on the distribution of dimensionless pressure. Adopting a smooth surface as the standard, transverse roughness increases P_{max}, while longitudinal roughness decreases P_{max}. With an increase in the power law index, using transverse roughness as an example, the shear thickening fluid (n=1.5) has the highest P_{max}, followed by Newtonian fluid (n=1.0) and shear thinning fluid (n=0.7).

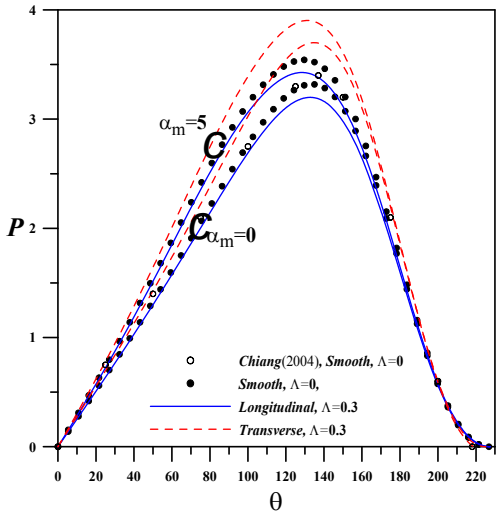

Fig. 4. Comparison between current simulations and those reported by Chiang [15] (Z=0, n=1, ε=0.4, λ=5, K=3)

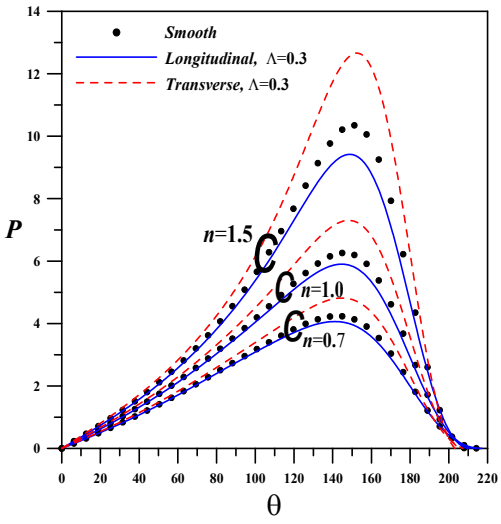

Fig. 5. Relationship between dimensionless pressure P and θ under the influence of various power law indices and surface roughness(ε=0.6, λ=5, α_m =5, K=3)

Table 1 illustrates the combined effects of surface roughness and a magnetic field according to variations in Pmax. When the magnetic field coefficient equaled zero, the maximum dimensionless pressure increased to 14.37%, in conjunction with an increase in transverse roughness from Λ=0 to Λ=0.3. In contrast, an increase in longitudinal roughness slightly decreased the maximum dimensionless pressure, compared to the smooth case. The current study assumed that the long journal bearings had a length-to-diameter ratio equal to 5; therefore, the axial variations in pressure were neglected in favor of those in the

Table 1. *P*max as a function of surface roughness various α_m(n=1, ε=0.6, λ=5, α_m=5, K=3)

Sureface roughness		Magnetic field coefficient α_m =0	$\frac{P_{max,\Lambda}-P_{max,\alpha_m=0,\Lambda=0}}{P_{max,\alpha_m=0,\Lambda=0}}\times100\%$	Magnetic field coefficient α_m =2	$\frac{P_{max,\Lambda}-P_{max,\alpha_m=0,\Lambda=0}}{P_{max,\alpha_m=0,\Lambda=0}}\times100\%$	Magnetic field coefficient α_m =5	$\frac{P_{max,\Lambda}-P_{max,\alpha_m=0,\Lambda=0}}{P_{max,\alpha_m=0,\Lambda=0}}\times100\%$
		P_{max}		P_{max}		P_{max}	
Longitudinal	Λ=0.3	5.531	-5.52%	5.648	-3.52%	5.879	0.43%
	Λ=0.1	5.816	0.6%	5.996	2.43%	6.182	5.60%
Smooth	Λ=0	**5.854**	0 %	6.053	3.40 %	6.324	**8.03 %**
Transverse	Λ=0.3	6.095	4.12%	6.296	7.55%	6.576	12.33%
	Λ=0.1	6.695	**14.37%**	7.092	21.15%	7.364	**25.79%**

circumferential direction. As a result, the transverse grooves generated stronger hydrodynamic lift, resulting in higher maximum dimensionless pressure; The influence of a magnetic field on maximum dimensionless pressure is presented in Table 1. Because the surface was assumed to be smooth, the maximum dimensionless pressure increased to 8.03% when the magnetic field coefficient was increased from 0 to 0.5. Finally, combining the influence of surface roughness and magnetic field resulted in a maximum dimensionless pressure of 25.79%, in the case of Λ=0.3 and α_m=0.5. It is clear that with an increase in the magnetic field, the influence of surface roughness is far more pronounced than that of a magnetic field and the coupled effects become more significant. To ensure strong hydrodynamic lift within the journal bearing and prevent side leakage caused by excessive hydrodynamic pressure, an appropriate balance must be attained between these two factors.

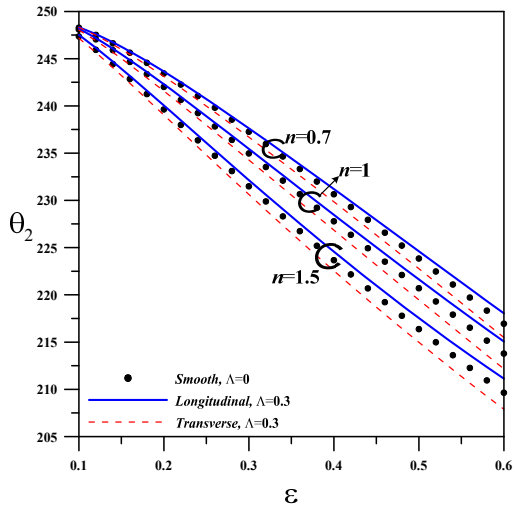

Fig. 6. Relationship between zero pressure gradient angle θ_2 and ε under various power law indices and surface roughness(λ=5, α_m=5, K=3)

Figure 6 illustrates the relationship between θ_2 and the eccentricity ratio ε under the influence of various power law indices. Obviously, when the journal bearing is operated using the same power law index, θ_2 reduces as the eccentricity ratio ε increases. Taking shear thickening fluid (n=1.5) as an example, transverse roughness reduced θ_2 by approximately 33° following an increase in eccentricity from 0.1 to 0.6. With the same roughness pattern, lower power law indices lead to higher θ_2. Thus, shear thinning fluids (n=0.7) produce higher θ_2.

The control circuit adjusts the timing alignment between the locally generated spreading signal and the received signal. When the timing alignment is correct, the correlator output will reach its maximal value. Therefore, the code acquisition can be attained by examining the peak locations of the correlator output signal.

Figure 7 exhibits the relationship between dimensionless load W and eccentricity ratio ε under various magnetic field coefficients. Clearly, dimensionless load is directly proportional to eccentricity ratio. The increase in dimensionless load resulting from an increase in the magnetic field coefficient is more apparent under conditions of low eccentricity ratio. Moreover, surface roughness patterns also have an influence on dimensionless load. Taking α_m=5 as an example, transverse roughness increases dimensionless load (compared with smooth bearing surfaces), whereas longitudinal roughness slightly decreases dimensionless load at a fixed eccentricity ratio.

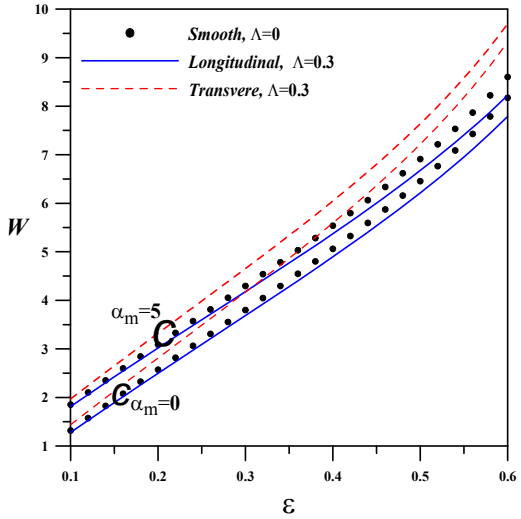

Fig. 7. Relationship between dimensionless load and eccentricity ratio under the influence of various magnetic fields and surface roughness(n=1, λ=5, α_m=5, K=3)

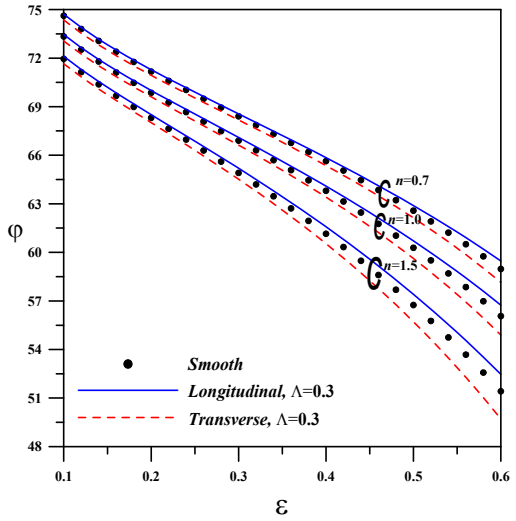

Fig. 8. Relationship between attitude angle and eccentricity ratio under the influence of various power law indices and surface roughness (λ=5, α_m=5, *K*=3)

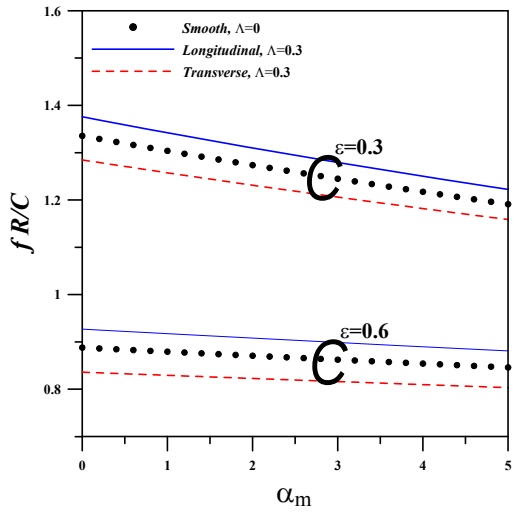

Fig. 9. Relationship between modified friction coefficient and magnetic field coefficient under various eccentricity ratios and surface roughness (*n*=1, λ=5, *K*=3)

Figure 8 illustrates the relationship between attitude angle φ and eccentricity ratio ε, under the influence of various power law indices. Clearly, the attitude angle was markedly reduced with an increase in eccentricity ratio. With a fixed power law index, the influence of roughness patterns on attitude angle grew with an increase in eccentricity ratio. Taking shear thickening fluid (n=1.5) as an example, longitudinal roughness reduced the attitude angle by approximately 21° when eccentricity increased from 0.1 to 0.6. With the same roughness pattern, lower power law indices lead to higher attitude angles. Thus, shear thinning fluids (n=0.7) produce higher attitude angles.

Figure 9 illustrates the relationship between the modified friction coefficient and the magnetic field coefficient under various eccentricity ratios. Taking ε=0.3 as an example, the modified friction coefficient shows a distinctively decreasing trend as the magnetic field coefficient increases. However, in the case of a high eccentricity ratio (ε=0.6), only a slight change is observed. Transverse roughness reduces the modified friction coefficient, whereas longitudinal roughness slightly increases the modified friction coefficient.

Figure 10 illustrates the relationship between the modified friction coefficient and roughness parameters under the influence of variations in the magnetic field. Using α_m=5 as an example, the modified friction coefficient associated with transverse roughness decreases as the roughness parameter increases; however, the modified friction coefficient associated with longitudinal roughness increases.

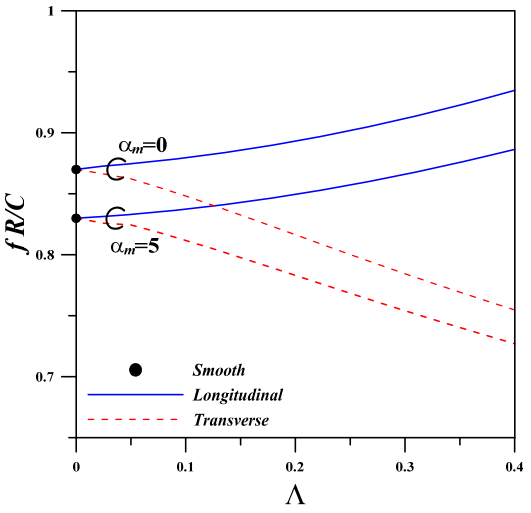

Fig. 10. Relationship between modified friction coefficient and surface roughness under the influence of various magnetic field coefficients and surface roughness (*n*=1, ε=0.6, λ=5, *K*=3)

IV. CONCLUSION

This study investigated the influence of lubricants containing suspended ferromagnetic particles on the lubrication characteristics of long journal bearings under the combined influence of a magnetic field and various surface roughness patterns. Using Christensen's stochastic surface roughness model and an infinitely long wire magnetic field model, we derived a Reynolds equation for long journal bearing approximation. The results obtained in other studies support the theoretical models outlined in this study and demonstrate the reliability of the proposed numerical analysis.

According to our results, the combined effect of surface

roughness and magnetic forces within bearings are significant and cannot be disregarded. Compared to bearings with smooth surfaces, the introduction of transverse roughness and a magnetic field can increase the film pressure and load capacity, while decreasing the attitude angle and modified friction coefficient. Longitudinal roughness has the opposite effect. The aforementioned trends become increasingly significant with an increase in the power-law index and eccentricity ratio. We believe that these simulation results will provide a valuable reference for the design of bearings in the future.

REFERENCES

1. Chiang, H.L., Lin, J.R., and Hsu, C.H., "Linear stability analysis of a rough short journal bearing lubricated with non-Newtonian fluids," *Tribology Letters*, Vol. 17, No. 4, pp. 867-877 (2004).
2. Chiang, H.L., Lin, J.R., and Hsu, C.H., "Lubrication performance of finite journal bearings considering effect of couple stresses and surface roughness," *Tribology International*, Vol. 37; pp. 297-307 (2004).
3. Chiang, H.L., Lin, J.R., Hsu, C.H., and Chang, Y.P., "Lubrication performance of long journal bearings considering effects of couple stresses and surface roughness," *Journal of the Chinese Institute of Engineers*, Vol. 27, No. 2, pp. 287-292 (2004).
4. Christensen, H., "Stochastic models for hydrodynamic lubrication of rough surface," *J. Proc. Instn. Mech. Engrs.*, Vol. 55, pp. 1013-1025 (1969-70).
5. Christensen, H. and Tonder, K., "The hydrodynamic lubrication of rough bearing surface of finite width," *ASME Journal of Lubrication Technology*, Vol. 93, pp. 324-330 (1971).
6. Chu, L.M., Li, W.L., Hsu, H.C., Chang, Y.P., "Magneto-elastohydrodynamic lubrication of circular contacts at impact loading", *Tribology International*, Vol. 42, pp. 333-339(2009).
7. Hsu, C.H., Lai, C., Lu, R.F., and Lin, J.R., "Combined effects of surface roughness and rotating inertia the squeeze characteristics of parallel circular disk," *Journal of Marine Science and Technology*, Vol. 17, No. 1, pp. 60-66 (2009).
8. Huang, W., Shen, C., and Wang, X., "Study on static supporting capacity and tribological performance of ferrofluid," *Tribology Transactions*, Vol. 52, pp. 717-723 (2009).
9. Katiyar, A., Singh, A.N., Shukla, P, Nandi, T., "Rheological of magnetic nanofluids containing spherical nanoparticles of Fe-Ni", *Powder Technology.*, Vol. 224, pp.86-89(2012).
10. Lin, J.R., Liang, L.J., and Chu, L.M., "Effects of non-Newtonian micropolar fluids on the squeeze-film characteristics between a sphere and a plate surface," *P I MECH ENG J-J TRIB*, Vol. 224, pp. 825-832 (2010).
11. Lin, J.R., "Derivation of ferrofluid lubrication equation of cylindrical squeeze films with convective fluid inertia forces and application to circular disks", *Tribology International*, Vol. 49, pp. 110-115(2012).
12. Montazeri, H., "Numerical analysis of hydrodynamic journal bearings lubricated with ferrofluid," *J. Intelligent Material Systems and Structures*, Vol. 222, No. 1, pp. 51-60 (2009).
13. Nada, G.S. and Osman, T.A., "Static performance of finite hydrodynamic journal bearings lubricated by magnetic fluids with couple stresses," *Triboogyl Letter*, Vol. 27, pp. 261-268 (2007).
14. Oladeinde, M.H. and Edokpia R.O., "Performance modeling of infinitely wide exponentially shaped slider bearing lubricated with couple stress fluids," *Journal of Engineering and Applied Science*, Vol. 5, No. 8, pp. 26-31 (2010).
15. Osman, T.A., Nada, G.S., and Safar, Z.S., "Static and dynamic characteristics of magnetized journal bearings lubricated with ferrofluid," *Tribology International*, Vol. 34, pp. 369-380 (2001).
16. Osman, T.A., Nada, G.S., and Safar, Z.S., "Different Magnetic models in the design of hydrodynamic journal bearings lubricated with non-Newtonian ferrofluid," *Tribology Letters*, Vol. 14, No. 3, pp. 211-223 (2003).
17. Osman, T.A., Nada, G.S., and Safar, Z.S., "Effect of using current-carrying-wire models in the design of hydrodynamic journal bearings lubricates with ferrofluid," *Tribology Letters*, Vol. 11, pp. 61-70 (2001).
18. Scott, W. and Suntiwattana, P., "Effects of Oil additives on the performance of a Wet Friction Clutch Material," *Wear*, Vol. 181-183, No. 2, pp. 850-855 (1995).
19. Sihuan, Y., Huang, W. and Wang, X., "Orientation effects of micro-grooves on sliding surface", *Tribology International*, Vol. 44, pp. 1047-1054 (2011).
20. Stokes, V.K., "Couple stress in fluids," *The physics of fluids*, Vol. 9, pp. 1709-1715 (1966).
21. Tarapov, I.E., *Magnetohydrodynamics*, Vol. 8, pp. 444 (1972).
22. Wang, X.L., Zhu, K.Q., and Wen, S.Z., "On the performance of dynamically loaded journal bearings lubricated with couple stress fluids," *Tribology International*, Vol. 35, pp. 185-191 (2002).